PROTEINS: Structure, Function, and Genetics 22:378–391 (1995)

Multiple Modes of Ligand Recognition: Crystal Structures of Cyclin-Dependent Protein Kinase 2 in Complex With ATP and Two Inhibitors, Olomoucine and Isopentenyladenine

Ursula Schulze-Gahmen,[1] Jeroen Brandsen,[1] Heather D. Jones,[2] David O. Morgan,[2] Laurent Meijer,[3] Jaroslav Vesely,[3,4] and Sung-Hou Kim[1]

[1]Department of Chemistry and Lawrence Berkeley Laboratory, University of California, Berkeley, California 94720, [2]Department of Physiology, University of California, San Francisco, California 94143-0444, [3]CNRS, Station Biologique, BP 74, 29682 Roscoff cedex, France, and [4]Department of Pathophysiology, Medical Faculty, University of Palacky, 775 15 Olomouc, Czech Republic

ABSTRACT **Cyclin-dependent kinases (CDKs) are conserved regulators of the eukaryotic cell cycle with different isoforms controlling specific phases of the cell cycle. Mitogenic or growth inhibitory signals are mediated, respectively, by activation or inhibition of CDKs which phosphorylate proteins associated with the cell cycle. The central role of CDKs in cell cycle regulation makes them a potential new target for inhibitory molecules with anti-proliferative and/or anti-neoplastic effects. We describe the crystal structures of the complexes of CDK2 with a weakly specific CDK inhibitor, N6-(Δ^2-isopentenyl)adenine, and a strongly specific inhibitor, olomoucine. Both inhibitors are adenine derivatives and bind in the adenine binding pocket of CDK2, but in an unexpected and different orientation from the adenine of the authentic ligand ATP. The N6-benzyl substituent in olomoucine binds outside the conserved binding pocket and is most likely responsible for its specificity. The structural information from the CDK2–olomoucine complex will be useful in directing the search for the next generation inhibitors with improved properties.**

Key words: X-ray crystallography, protein kinase inhibitors, CDK inhibitor specificity, cancer, drug design

INTRODUCTION

The timing and integration of the eukaryotic cell division and growth cycle are controlled by cyclin-dependent kinases (CDKs),[1] which are highly conserved among eukaryotic species. Higher eukaryotic cells contain several isoforms of CDKs that become activated in specific phases of the cell cycle. CDKs are able to phosphorylate many proteins that are involved in cell cycle events, including histones, lamins, and tumor suppressor proteins like the retinoblastoma gene product pRb.[1–3] In accordance with their central role in the cell cycle, enzyme activity is tightly controlled by multiple mechanisms. Kinase activation requires complex formation with regulatory cyclin proteins, followed by an activating phosphorylation on Thr-161 in CDC2 or the corresponding Thr in other CDKs.[4–8] In addition, enzyme activity is negatively regulated by phosphorylations at Tyr-15 and/or Thr-14[6,7,9–12] or by complex formation with inhibitor proteins like p16[13–15] p27,[16,17] p28,[18] and p21,[19–22] the latter being inducible by p53. Especially noteworthy is the fact that deletions of the p16 gene were found in over 50% of all human malignant cell lines tested,[14,15] although much less in primary tumor cells,[23] implicating p16 functions as tumor suppressor protein. Thus, both the cell growth signals transmitted through many oncogene products and the growth inhibitory signals from several tumor suppressor proteins modulate the activity of CDKs. Although mutations in CDKs themselves have not been associated with cancer, cyclin overexpression has been linked to tumorigenesis.[24–26] Hence, CDKs are a promising target for developing inhibitors with antineoplastic effects and for the treatment of cell-proliferative diseases.

By screening purine analogs for specific protein kinase inhibitors of CDKs, Vesely et al. found olomoucine to specifically inhibit CDC2/cyclin A, CDC2/cyclin B, CDC2/cyclin E, CDK2/cyclin A, CDK2/cyclin E, the brain CDK5/p35, and mitogen activated protein (MAP) kinases.[27] Here we describe the X-ray structure of CDK2 in complex with olomoucine and a weakly specific inhibitor N6-(Δ^2-isopentenyl)adenine (iP). A comparison with the

Received December 19, 1994; revision accepted February 6, 1995.

Address reprint requests to Sung-Hou Kim, Department of Chemistry and Lawrence Berkeley Laboratory, University of California, Berkeley CA 94720.

J. Brandsen is on leave from the Department of Crystal and Structural Chemistry, University of Utrecht, Utrecht, The Netherlands.

TABLE I. Diffraction Data Collection Statistics of CDK2 Complexes

Inhibitor	Olomoucine		Isopentenyladenine	
Space group	$P2_12_12_1$		$P2_12_12_1$	
Cell dimensions	a = 73.77 Å		a = 73.25 Å	
	b = 72.55 Å		b = 72.51 Å	
	c = 54.06 Å		c = 54.03 Å	
Number of measurements	50,892		134,195	
Unique reflections	15,044		25,371	
Data completeness	∞–2.5 Å	99.0%	∞–2.0 Å	96.4%
	2.5–2.2 Å	97.0%	2.0–1.8 Å	84.0%
R_{sym} on intensity*	8.4%		8.3%	

*$R_{sym} = \Sigma \mid I(h) - \langle I(h) \rangle \mid / \Sigma I(h)$, with $I(h)$, observed intensity and $\langle I(h) \rangle$, mean intensity of reflection h over all measurements of $I(h)$.

X-ray structure of the ATP–CDK2 complex,[28] and with other available kinase structures can explain the selectivity of olomoucine and provides structural information for further improvement of the inhibitor affinity and specificity.

MATERIALS AND METHODS

Human CDK2 was prepared as described in Rosenblatt et al.[29] N6-(Δ^2-isopentenyl)adenine was obtained from Sigma Chemicals and olomoucine, 2-(2-hydroxyethylamino)-6-benzylamino-9-methylpurine, was obtained from ACDC Research Laboratories [3724 TM 1960 WEST, Suite 310, HOUSTON, Texas 77068, U.S.A., fax (1) 713.397.6031].

Cocrystallization and Inhibitor Soaking

Crystals of CDK2 complexes with various ligands were obtained either by cocrystallization under crystallization conditions for CDK2 apoprotein[19] or by soaking crystals of CDK2 apoprotein in ligand-containing solutions, or in both ways.

The Mg^{2+}-ATP–CDK2 complex was obtained by soaking CDK2 crystals in a 50 mM HEPES buffer, pH 7.4, containing 2.5 mM $MgCl_2$ and 1.25 mM ATP.[28] These crystals diffracted to 2.0 Å resolution. Cocrystallizations with ATP under the same conditions were also successful, yielding crystals with identical space group ($P2_12_12_1$) and cell dimensions as the apoenzyme crystals. Since the crystals obtained by cocrystallization diffracted to slightly lower resolution, we will refer to the ATP-soaked crystal structure for the following analysis.

Because iP and olomoucine are poorly soluble in water, very small amounts of solid inhibitor were introduced using a hair into the crystalization drops containing CDK2 protein. Cocrystals of CDK2 with the weakly specific protein kinase inhibitor, iP, could be obtained both by cocrystallization and soaking. The iP–CDK2 complex structure described here was obtained from a soaking experiment and the crystals diffracted to at least 1.8 Å. In contrast, crystals of the CDK2–olomoucine complex could only be obtained by cocrystallization since soaking native CDK2 crystals with olomoucine cracked the crystals. The complex crystals grow as chunky plates of average dimensions 0.6 × 0.3 × 0.1 mm, different from the diamond or block shaped native crystals (0.8 × 0.5 × 0.4 mm). Although the CDK2–olomoucine complex crystals had a different morphology than the apoenzyme crystals, they grew in the same space group with the same cell dimensions within the margin of errors.

Data Collection and Refinement

Data for all CDK2 complex crystals were collected at room temperature using a Rigaku RAXIS-II imaging plate area detector and processed with the Raxis data processing software (Table I). Merging the diffraction data of the complex and apocrystals with CMBISO from the program package PHASES[30] resulted in R_{scale} values on intensities of 0.18 for the iP complex and of 0.29 for the olomoucine complex.

Refinement of both CDK2–inhibitor complexes proceeded with refining the position of the native CDK2 model including its water structure as rigid body against the complex data, using XPLOR 3.1.[31] The R-value for the iP complex was reduced from 0.38 to 0.26 with data from 8.0 to 1.8 Å resolution. A much larger decrease from 0.49 to 0.26 for the olomoucine complex with 10.0 to 3.5 Å data is indicating a slightly different packing arrangement from that of the CDK2–apoenzyme crystals. At this stage, $F_o - F_c$ maps with σ_A weighting[32] were calculated with water molecules in the ATP binding pocket omitted for F_c calculations. These maps showed clear density for both inhibitors. The conformation of residues forming the binding pocket was checked in simulated annealing omit maps before including the inhibitor molecules in the complex structures. Further refinement in XPLOR continued with simulated annealing using the slow-cooling protocol,[33] followed by alternate cycles of positional refinement and manual rebuilding of the complete structures into simulated annealing omit maps using TOM and FRODO.[34] Of the protein structure 5–10% was omitted for each map calculation. Finally, the positions of water molecules were checked and corrected in $F_o - F_c$ omit maps, for which all water molecules

TABLE II. Refinement Statistics for CDK2 Complex With Inhibitors

Inhibitor	Olomoucine	Isopentenyladenine
Resolution (Å)	8.0–2.2	8.0–1.8
R-value*	0.19	0.20
R-free†	0.27	0.27
rmsd from ideal bond length (Å)	0.013	0.011
rmsd from ideal bond angle (°)	1.70	1.76
B-average‡	31	30
Number of water molecules	76	99

*$R = \Sigma |F_o - F_c| / \Sigma F_o$ with $F/\text{sig}F > 2$ cutoff.
†*R*-free = *R*-value for 10% of the data, which were not included during crystallographic refinement.
‡Average *B*-value for all nonhydrogen protein atoms.

were omitted for F_c calculations. Water molecules were modelled into difference densities larger than 3σ if hydrogen bonding partners were available at the correct distance and angle. The final models have *R*-values of 0.20 for the iP complex and 0.19 for the olomoucine complex with restrained individual *B*-values and good stereochemistry (Table II).

Analysis of the Structures

Rms differences on backbone atoms were calculated with the Protein Analysis Package (PAP).[35] Proteins were superimposed on Cα atoms using the program OVRLAP[36] with the simple progression rule. This allows the refinement of equivalent residues in two homologous proteins, followed by the refinement of the transformation to obtain the best fit of equivalent Cα atoms.

Hydrogen bonds and van der Waals contacts were assigned with the program CONTACSYM.[37] The cutoff for hydrogen bonds and salt bridges was 3.4 Å and up to 4.11 Å for van der Waals contacts, depending on the atom type and using standard van der Waals radii. The solvent accessibility of individual residues was assessed using the program MS[38] with a 1.7 Å radius for the solvent probe.

RESULTS

Overall Protein Conformation

The crystal structure of apo-CDK2 and its complex with ATP have been described recently.[28] We have now solved the structures of the same enzyme with two inhibitors, isopentenyladenine which is a relatively nonspecific protein kinase inhibitor, and olomoucine, which is a specific inhibitor for CDC2, CDK2, CDK5, and MAP kinases (Table III, Fig. 1).[27]

The CDK2–iP and CDK2–olomoucine complexes have been determined to high resolution (1.8 and 2.2 Å), with good stereochemistry (Table II). As in the apoenzyme and in the CDK2–ATP complex, electron density is weak for two regions in the enzyme spanning residues 37–43 and 153–163. These segments have been omitted in the olomoucine complex structure because of very weak and fragmented density. In the iP complex, these residues could be placed into density, but high temperature factors in the region 152–163 (between 54 and 89 Å^2 on Cα) indicate high flexibility of this loop region which is part of the "T-loop"[28] containing the activating Thr-160 phosphorylation site. A few residues in these loops also adopt unfavorable conformations in Φ/Ψ space. Otherwise, the Ramachandran plots[39] for both inhibitor complexes show tight clustering of peptide conformations in the energetically favorable regions with only one residue, Arg-126, just outside the favorable area.

As expected from the fact that both inhibitor complexes crystallize in the same space group with nearly identical cell dimensions as the apoenzyme and the ATP complex, we observe very similar backbone conformations. The enzyme is folded into the typical bilobal structure, with the smaller N-terminal domain consisting predominantly of β-sheet structure and the larger C-terminal domain consisting primarily of α-helices. There are no significant differences in the domain orientations between the inhibitor–enzyme complexes and the ATP–enzyme complex, and the inhibitors bind, like ATP, in the deep cleft between the two domains (Fig. 2). Root mean square (rms) differences for all backbone atoms among the CDK2–iP complex, the CDK2–ATP complex, and the apoenzyme are small, ranging from 0.26 to 0.35 Å, whereas rms differences between the CDK2–olomoucine complex and all other CDK2 structures range from 0.56 to 0.60 Å. The highly flexible regions 37–43 and 153–163 were excluded from these calculations. The larger rms differences in the olomoucine complex are mainly due to the N-terminal 30 residues in β-strands 1 and 2, which form part of the binding pocket provided by the small domain.

Geometry of Ligand Binding

Isopentenyladenine and olomoucine are purine derivatives. The electron density for all atoms of the inhibitors is clear and strong (Fig. 3a and b). Although the purine rings bind roughly in the same area of the binding cleft as the adenine ring of ATP, the orientation of the purine ring with respect to the protein is different in all three ligands. This is probably due to the different size of the substituent

TABLE III. Inhibitory Effect of Olomoucine and Isopentenyladenine on Various Purified Protein Kinases*

Enzyme	IC_{50} (μM)	
	Olomoucine	Isopentenyladenine
$p34^{cdc2}$/cyclinA	~50	—†
$p34^{cdc2}$/cyclinB	7	45
$p34^{cdc2}$/cyclinE	~10	—
$p33^{cdk2}$/cyclinA	7	50
$p33^{cdk2}$/cyclinE	7	—
$p34^{cdk4}$/cyclinD	>1000	200
$p33^{cdk5}$/p35	3	80
$p40^{cdk6}$/cyclin D3	>250	>100
$p44^{mpk}$‡	25	95
GST-erk-1‡	30	90
Protein kinase C, various isozymes	≥1000	43–>100
Cyclic AMP-dependent kinase	>2000	50
Cyclic GMP-dependent kinase	>2000	50
Calmodulin-dependent kinase II	no effect	—
Myosin light chain kinase	>1000	>1000
Mitogen-activated S6 kinase ($p70^{s6k}$)	no effect	—
Casein kinase 2	>2000	600
dsRNA-activated protein kinase (PKR)	>500	>1000
$p56^{lck}$	>2000	90
$p56^{lyn}$	>1000	>2000
TPKIIB‡	>1000	>2000
$p55^{fgr}$(TPK-III/Q1)‡	>1000	78
c-*src*	no effect	1000

*This table is a summary of Table 1.[27]
†—, not tested.
‡mpk, mitogen-activated protein kinase; GST-erk-1, glutathion *S*-transferase-extracellular signal regulated kinase 1; TPK, tyrosin protein kinase.

groups in the three ligands; the N6 amino group of the adenine ring is replaced by an isopentenylamino group in iP and by a bulky benzylamino group in olomoucine (Fig. 1). Since the adenine of ATP binds with the N6 amino group pointing into the deepest part of the cleft (Fig. 4), this orientation is sterically impossible for the inhibitors with their larger N6 side chains. However, both inhibitors lack large substituents at the N9 position of the purine ring which could substitute for the ribose and phosphate atoms in ATP. Hence one mode of inhibitor binding, observed for iP, is obtained by rotating the purine ring about 180° around an axis through the N3 and N7 atoms of the purine rings (Fig. 5b). In this orientation, the N6 atom now points away from the deep pocket, allowing the isopentenyl group on N6 to bind in the binding pocket area occupied by the ribose in ATP (Fig. 4).

For the olomoucine complex, we observe still another orientation of the purine ring (Figs. 4 and 5c). The hydroxyethyl group on N2 binds to an area of the binding pocket occupied by the ribose in the CDK2–ATP complex, and the N6 benzyl group binds between β-strand 1 and the β5–α2 connecting loop, which bridges the small and large domains of CDK2 (Figs. 2 and 4). Since the benzyl group is the only part of olomoucine that binds outside the conserved binding pocket, it is most likely responsible for the specificity of olomoucine for CDKs.

CDK2 interactions with ATP are characterized by predominantly hydrophobic and van der Waals interactions to the adenine base and ionic interactions, hydrogen bonds, and van der Waals interactions with the ribose and triphosphate of ATP (Fig. 6a). In total, there are 26, 15, and 38 contacts between CDK2 and the adenine base, ribose, and phosphates, respectively. The adenine ring is enclosed in a hydrophobic pocket formed by Ile-10, Ala-31, Val-64, Phe-80, Phe-82, and Leu-134 (Fig. 6a) and forms two hydrogen bonds, between the N6 atom of adenine and the carbonyl oxygen of Glu-81, and between N1 and the backbone amide of Leu-83. These hydrogen bonds are conserved in the cyclic AMP-dependent kinase (cAPK)[40,41] and the bond to N6 has been shown to be important for binding affinity.[42]

Since both inhibitor molecules are quite hydrophobic, their binding to CDK2 is characterized by predominantly hydrophobic and van der Waals interactions with the same hydrophobic enzyme residues that form the pocket for the adenine base. However, because of the different purine orientations, the contacts are formed with different atoms in the purine rings. In addition, the extent to which indi-

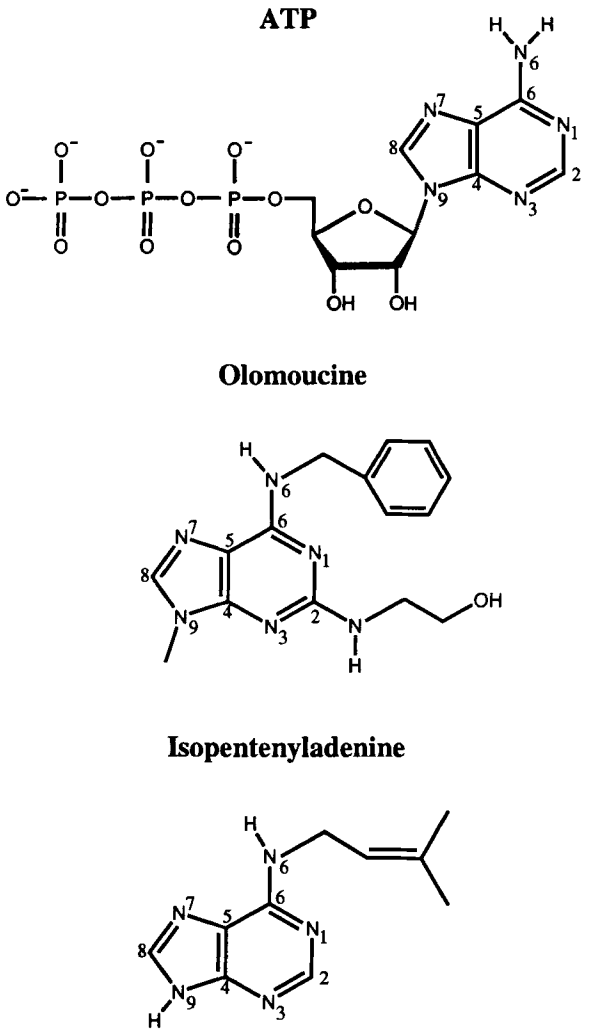

Fig. 1. Chemical structures of three CDK2 ligands. The inhibitors olomoucine and isopentenyladenine bind competetively with the natural ligand ATP.

vidual enzyme residues contribute to ligand binding varies between the complexes. In the iP complex, the hydrophobic contacts to the purine are spread quite evenly among the contact residues. The number of contacts with the purine (28) is similar to what is seen in the ATP complex (26) and includes 3 hydrogen bonds (Fig. 6b), two of which are formed with the same enzyme residues (Glu-81O, Leu-83N) that form hydrogen bonds to the adenine base in the ATP complex. The isopentenyl group adds 8 more van der Waals contacts to the enzyme increasing the total number of contacts between iP and CDK2 to 36.

In the olomoucine–CDK2 complex, the purine ring atoms form a total of 36 contacts, with only two enzyme residues, Ile-10 and Leu-134, providing 44% of the contact atoms. As in the iP and ATP complex, Leu-83N is hydrogen bonded to the purine ring, but Glu-81O appears to have no hydrogen bonding partner in the CDK2–olomoucine complex. An additional hydrogen bond is formed between Leu-83O and the N6 atom. The hydroxyethylamino side chain in olomoucine contributes only 5 contacts with the protein and, hence, is probably not very important for binding affinity. In contrast, the N6 benzyl side chain in olomoucine participates in a total of 16 contacts, 7 with ILe-10, 1 with the Phe-82 side chain, 5 with backbone atoms of residues 83–85, 2 with the side chain of Lys-89, and 1 with the Leu-134 side chain. In addition, the geometry of the Lys-89 benzene interaction is typical for a hydrogen bond with an aromatic ring.[43,44]

Since the key contact residues to olomoucine, Ile-10 and Leu-134, are conservatively replaced among kinases and many of the remaining benzyl contacts are with backbone atoms, it is difficult to identify one or a few protein residues that are critical for olomoucine specificity from sequence comparisons alone. Structural differences caused directly or indirectly by conservative replacements of Ile-10 or Leu-134 or sequence differences in the less conserved residues Phe-82 to Lys-89 could be the basis for the binding specificity of olomoucine. In addition, sequence insertions and terminal extensions in other kinase structures could sterically interfere with olomoucine binding.

Buried Surface Areas

The specificity and affinity of protein ligand complexes depends on directional hydrogen bonds, ionic interactions, as well as on shape complimentarity of the contact surfaces of both partners.[45,46] These are best described as solvent-accessible surfaces that become buried upon ligand binding. In the CDK2–ATP complex, the buried surface areas of ATP (352 Å^2) and CDK2 (435 Å^2) show a close fit. ATP is almost completely inaccessible to solvent and its buried surface amounts to 80% of the buried surface in CDK2.

The inhibitor–CDK2 complexes show good complementarity in the area of the purine ring but the fit for the much smaller groups substituting for the ribose and phosphates in ATP is less optimal (Fig. 7a and b). Although the inhibitors are almost completely solvent inaccessible, parts of the binding pocket involved in phosphate and ribose binding remain solvent accessible. The buried surfaces for the olomoucine and iP complexes are smaller than for the ATP complex with 261 and 360 Å^2 for olomoucine and CDK2, and 203 and 290 Å^2 for iP and CDK2, respectively.

Differences in Protein Side-Chain Conformations in the Binding Pocket

To find out if inhibitor binding to CDK2 induces changes in side chain conformations in the binding pocket, we compared the structures of the binding pockets of CDK2–ATP complexes and CDK2–inhib-

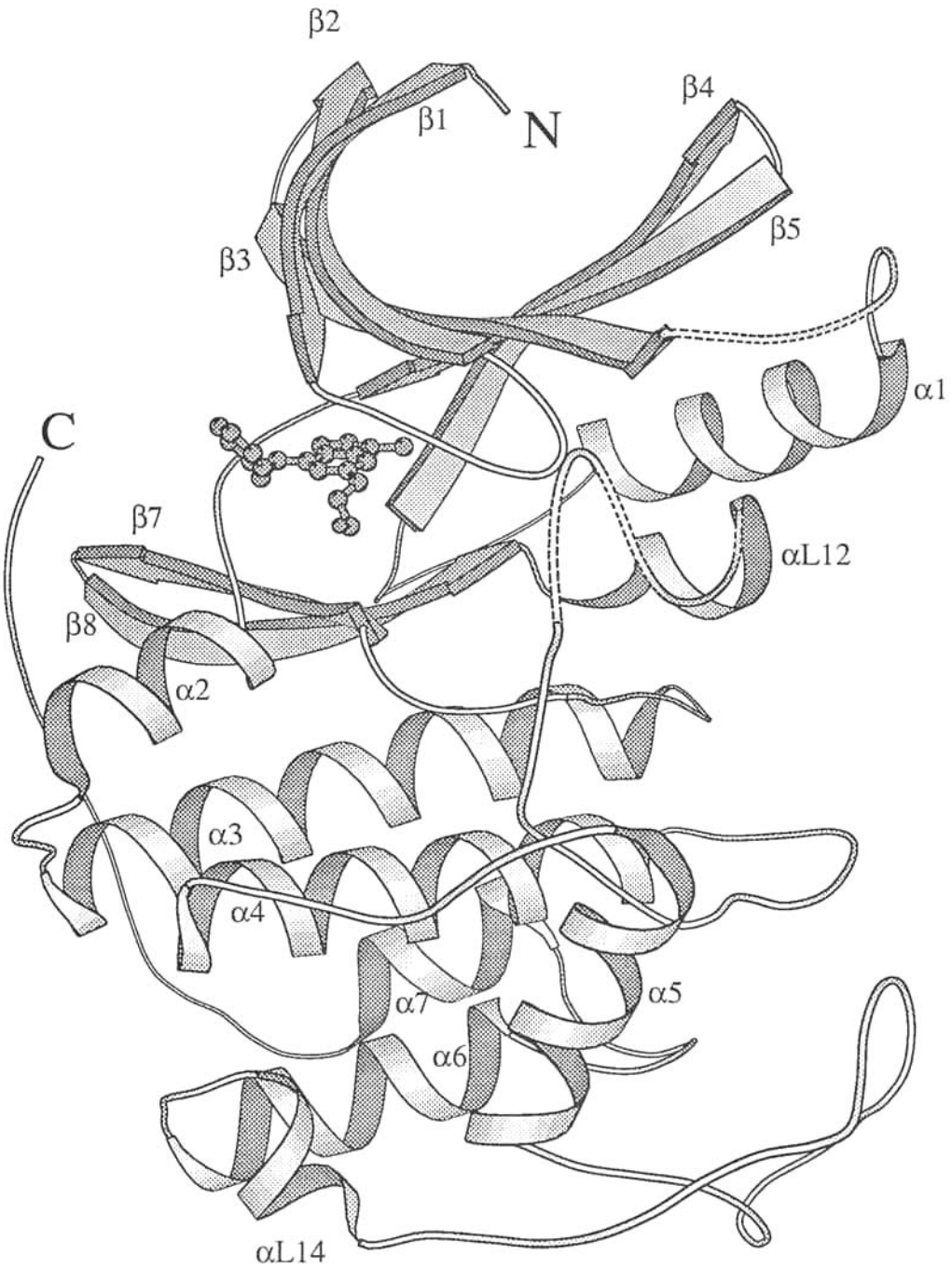

Fig. 2. Schematic drawing of CDK2 with the inhibitor olomoucine superimposed in the binding pocket between the smaller N-terminal domain and the larger C-terminal domain. Secondary structural elements are indicated by arrows for β-strands and coils for α-helices, and labeled as in the apoenzyme.[28] Residues 37–43 and 153–163 which have weak electron densities are drawn with dotted lines.

itor complexes after superposition of the enzyme on Cα atoms. Several side chains show significant conformational differences among these complexes (Fig. 4). The Ile-10 side chain in the olomoucine complex, which has well defined electron density, is rotated by 120° in χ_1 relative to the side chain conformation in the other two complexes. Since this residue forms a larger number of hydrophobic contacts with the benzylamino group of olomoucine and the purine ring, its conformational change is most likely induced by olomoucine binding. In addition, Ile-10 is located N-terminal to the glycine-rich loop

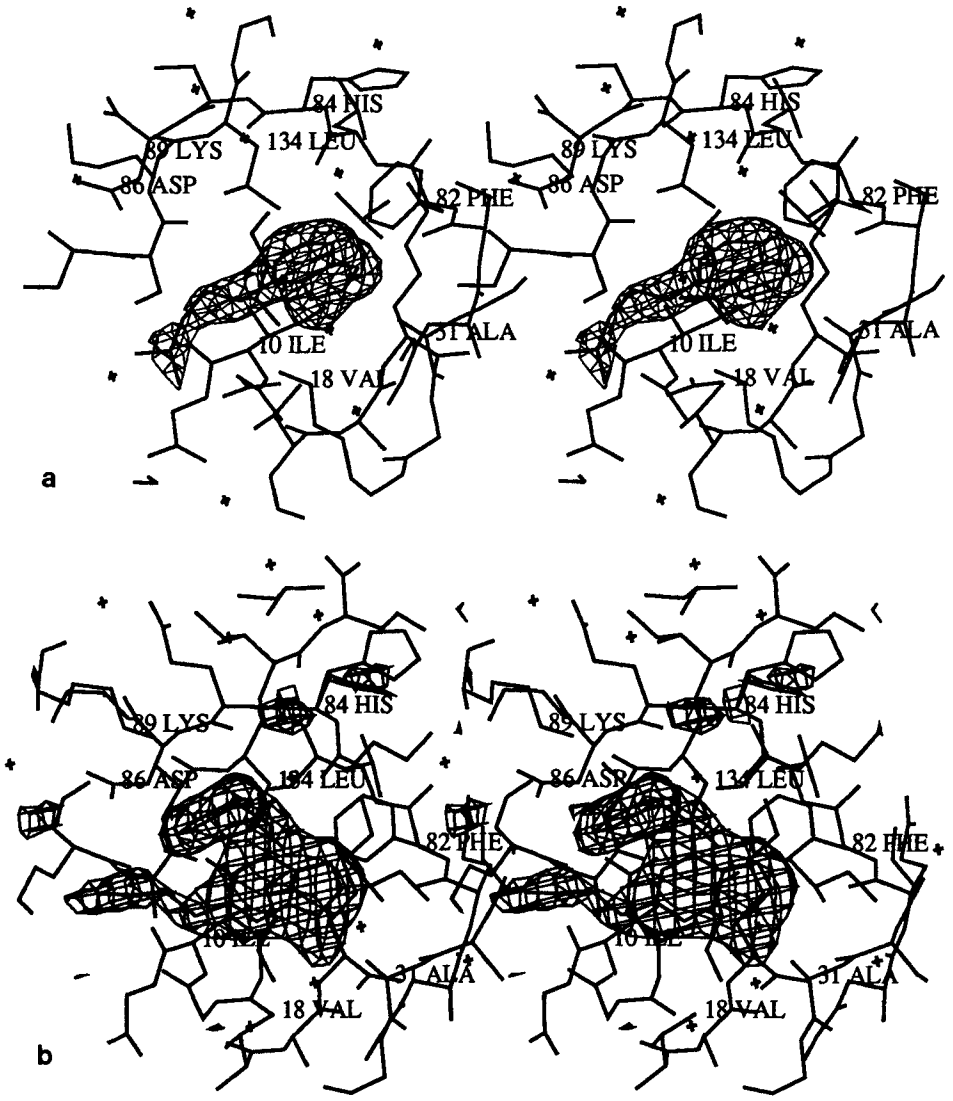

Fig. 3. Stereo view of the electron density for isopentenyladenine (**a**) and olomoucine (**b**) in difference electron density maps calculated after simulated annealing refinement of CDK2 apoprotein. The maps are contured at 3.5σ and 3.0σ, respectively, and displayed with FRODO.[34] Some residues forming the ligand binding site are labeled.

(residues 11–16) that contacts the phosphate atoms in the ATP complex and shows increased rms deviations for backbone atoms in the olomoucine complex. Hence, these backbone differences could be influenced by the Ile-10 olomoucine contacts.

Lys-33 and its equivalent Lys-72 in cAPK are important for ATP binding. In the CDK2–ATP complex, Lys-33 forms salt bridges with the α phosphate of ATP and Asp-145, another residue involved in ATP-Mg^{2+} binding.[28] The side chain conformation of Lys-33 in the olomoucine complex is very similar to the ATP complex, but in the iP complex, it moves closer toward the inhibitor. The Nϵ moves by 2.8 Å relative to the ATP complex structure and forms 4 contacts with the edge of the purine ring including a hydrogen bond with N7.

The side chain of Gln-131 is directed away from the binding pocket in the ATP and iP complex. In the olomoucine complex, however, the side chain points into the binding pocket and forms van der Waals contacts and a hydrogen bond with the hydroxyethylamino group of olomoucine. The following residue, Asn-132, adopts the same conformation in the apoenzyme and inhibitor complexes. Its side chain amide hydrogen bonds with the backbone carbonyl oxygen of residue 129, whereas in the ATP–CDK2 complex, the side chain is rotated into the binding pocket and forms hydrogen bonds with the Mg^{2+} ion as well as with β and γ phosphate oxygens.

In summary, the observed side chain differences in the binding pocket seem to contribute to an im-

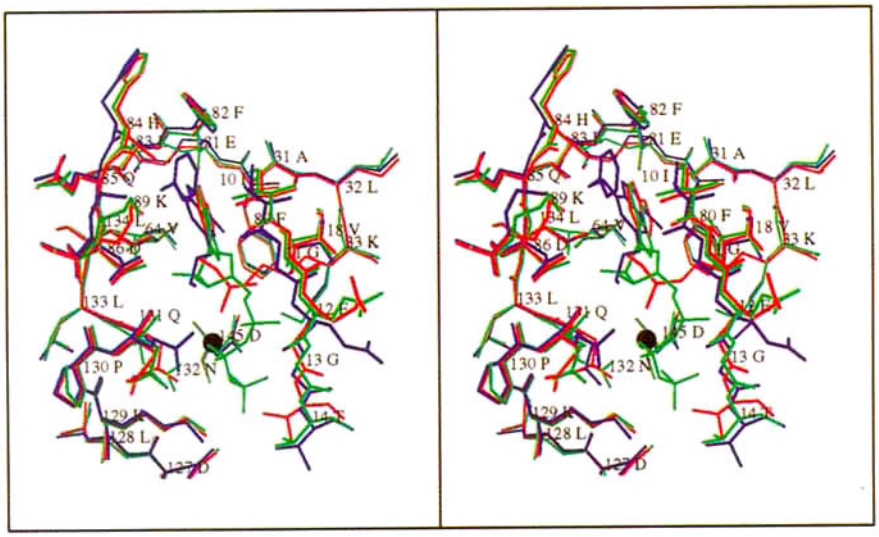

Fig. 4. Stereo drawing of the superimposed binding pockets of the CDK2–ATP complex and CDK2–inhibitor complexes. The ATP complex is shown in green with the Mg^{2+} atom as black sphere. The isopentenyladenine complex and olomoucine complex are drawn in red and blue, respectively.

proved fit between protein and ligand molecules. Conformational differences in a few other side chains in the binding pocket are probably not significant since high *B*-values and weak or missing electron densities indicate high flexibility for those residues.

DISCUSSION

The high resolution X-ray structures of human CDK2 in complex with two small inhibitor molecules, iP and olomoucine, provide data to analyze the structural basis of specific inhibition by comparison with the CDK2–ATP complex[28] and other known protein kinase structures. Since ATP binding to CDKs has not been well characterized biochemically, and ATP binding pockets are structurally conserved between CDK2 and cAPK,[41,47] we will compare our data with binding studies of ATP analogs to the catalytic subunit of cAPK.[42,48]

These earlier studies indicated that most of the binding affinity is contributed by the adenine ring since the K_D for ATP (10 μM), ADP (10 μM), and adenosine (35 μM) binding to cAPK[48] are very similar. However, large increases in K_D for ATP analogs with replacement of N6 by a keto group or a benzylamino group, and for analogs with a chlorine atom at position 2 of the adenine base were observed. These results are understandable because the crystal structure of the ATP–CDK2 complex shows very little space around the N6 and C2 atom of adenine, and the N6 atom is a hydrogen donor in a conserved hydrogen bond with the carbonyl oxygen of Glu-81. Therefore, it was a surprise to find that olomoucine and iP, both having large substituents on N6, are competetive inhibitors for ATP with apparent inhibition constants of 14 and 78 μM, respectively.[27] The crystal structures of the CDK2 complexes with the inhibitors reveal that their adenine moieties bind in the same binding pocket as the adenine of ATP, but with completely different orientations of the purine ring (Fig. 5). These different binding orientations allow accommodation of the large substituent groups, but lead also to changes in hydrogen bonds between CDK2 and purine atoms. The hydrogen bond from Glu-81 O to N6 in ATP (Fig. 6a) is substituted by a hydrogen bond to N9 in the iP complex (Fig. 6b) and it is lost completely in the olomoucine complex (Fig. 6c). Instead a different hydrogen bond between Leu-83N and the purine N7 is formed, that is not found in the ATP or iP complexes. This hydrogen bond together with 5 van der Waals contacts from the olomoucine N7 atom to CDK2 residues explain why substitutions at N7 completely abolish inhibitory activity.[27] However, with only 3 hydrogen bonds out of 57 total contacts between olomoucine and CDK2 (36 in the iP complex), most of the binding affinity can probably be attributed to van der Waals contacts and hydrophobic interactions.

Although the inhibitors and ATP are found in completely different orientations in the binding pocket, the structural differences between the binding pockets are relatively small. Only the olomoucine complex shows a significant difference to all other CDK2 structures in the backbone atoms of residues 1–29 with rms deviations per residue between 0.4 and 2.0 Å. These residues include β-strands 1 and 2 and the connecting glycine-rich loop which forms a flap that lines the interdomain binding pocket for ATP. In the olomoucine complex, the flap

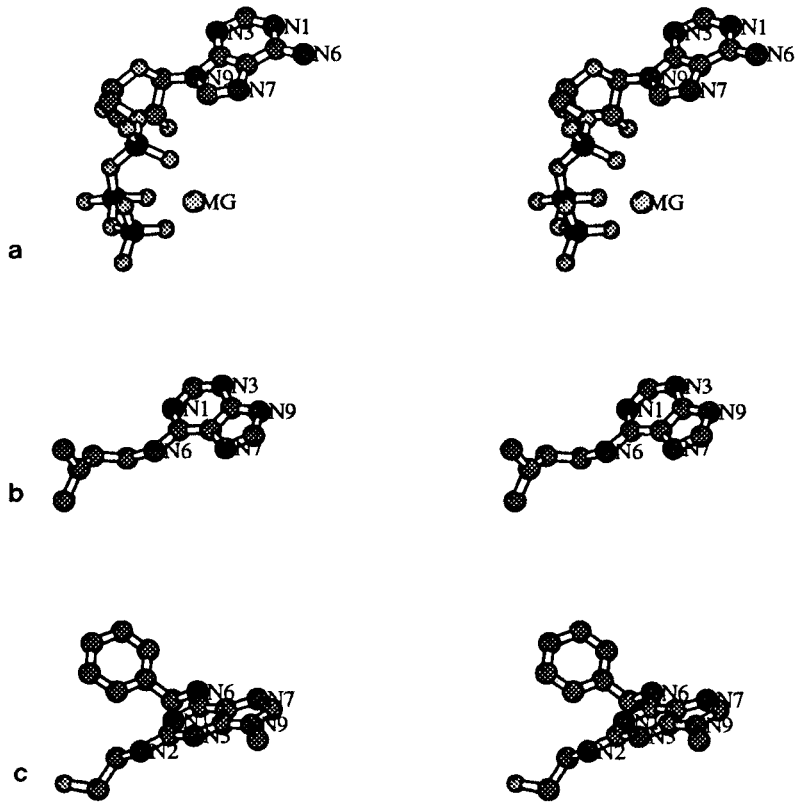

Fig. 5. Stereo drawing of CDK2 ligands after superimposition of the complex structures on Cα atoms of CDK2. The orientation of the purine rings in the three ligands, ATP (**a**), isopentenyladenine (**b**), olomoucine (**c**), is very different, most likely as a result of the different size and location of substituent groups in the purine ring.

in the small lobe moves towards the large domain, thereby further closing the binding pocket. This movement could be caused by the lack of a large side chain in olomoucine that can substitute for the ribose and phosphate groups in ATP. In the complex with iP, which has the larger isopentenyl side chain in the ribose binding area, the flap position resembles more closely the ATP complex. In addition, conformational differences in Ile-10 induced by olomoucine binding might influence the position of backbone atoms in β-sheets 1 and 2 and the glycine-rich loop.

Adjustment of side chain conformations in residues Ile-10, Lys-33, Gln-131, and Asn-132 improves the complementarity of ligand and enzyme surfaces in all three complexes. Especially interesting is the conformational change in Ile-10 in response to olomoucine binding. The side chain conformation of Ile-10 in the ATP complex would have unfavorably close van der Waals contacts with the benzylamino group of olomoucine. A rotation of 120° in χ_1 relieves these bad contacts in the olomoucine complex and results in 7 van der Waals contacts with the benzylamino group. Since Ile-10 is conserved or conservatively replaced by Val or Leu residues in all other known protein kinases, we energy minimized the CDK2 structure with an Ile to Leu replacement in position 10 using XPLOR.[31] The minimized CDK2-Leu-10 structure provides less favorable contacts to olomoucine. Similarly, CDK2 with a valine in position 10 would lose favorable contacts provided by the ILe Cδ atom. Hence, Ile seems to be the best contact residue for olomoucine in this position.

Vesely et al.[27] showed that olomoucine is a good inhibitor for most CDKs and also for ERK1-MAP kinase, which is 90% identical to ERK2-MAP kinase, but not for cAPK (Table III). To identify structural differences that could account for the specificity of olomoucine, we superimposed the olomoucine–CDK2 complex (Fig. 8a) onto the known three-dimensional structures of cAPK[49] and ERK2-MAP kinase.[50] Positioning of olomoucine in cAPK from the ternary complex with Mg^{2+}-ATP and peptide inhibitor leads to a complete overlap of the Phe-327 side chain in the C-terminal extension of cAPK and the benzylamino group of olomoucine (Fig. 8b). Although the C-terminal segment 317–340 adopts a different conformation in one crystal form of the binary complex of cAPK with peptide inhibitor,[51] this sterical clash in the active form of the enzyme most

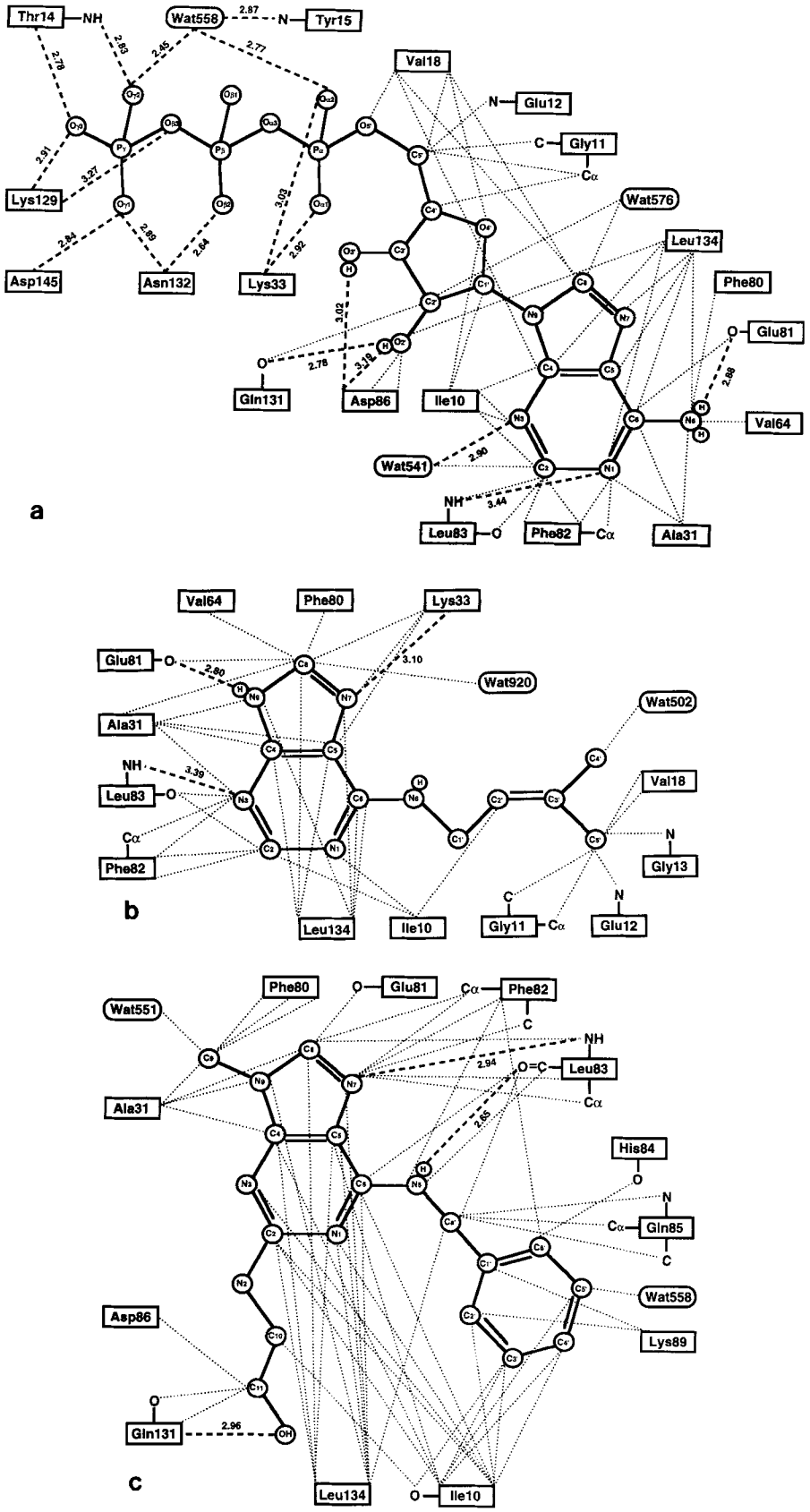

Fig. 6. Schematic drawing of CDK2 interactions with ATP (**a**), isopentenyladenine (**b**), and olomoucine (**c**). Protein side chain contacts are indicated by lines connecting to the respective residue box while interactions to main chain atoms are shown as lines to the specific main chain atoms. Van der Waals contacts are indicated by dotted lines, and hydrogen bonds by broken lines. For the inhibitors (**b,c**), all ligand contacts are shown, while for ATP, van der Waals contacts to phosphates were omitted for clarity.

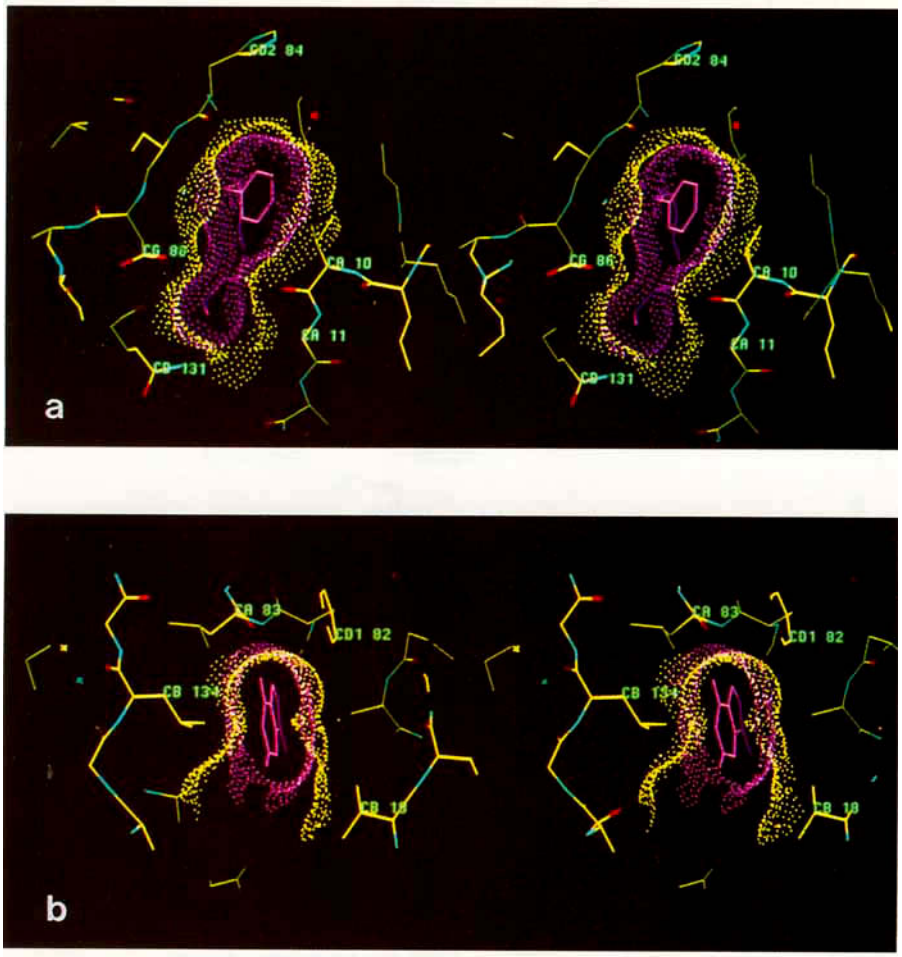

Fig. 7. Buried surface areas of CDK2 (yellow) and olomoucine (purple) in the CDK2–olomoucine complex. Solvent inaccessible surfaces were calculated with a solvent probe of 1.7 Å radius and displayed as dot surfaces using TOM.[34] A cross-section through the complex at the level of the benzylamino group and the purine ring of olomoucine are shown in (**a**) and (**b**), respectively.

likely prevents olomoucine binding to and hence inhibition of cAPK.

Placing olomoucine into the ERK2-MAP kinase structure causes no unfavourable sterical contacts (Fig. 8c). In ERK2, the C-terminal extension to the catalytic core is located on the enzyme surface away from the binding pocket and hence does not interfere with ligand binding. Four out of 7 residues that form contacts with the benzyl group in CDK2 have similar contacts in ERK2. The side chains of Ile-29 and Lys-112, corresponding to Ile-10 and Lys-89 in CDK2, and main chain atoms of residues 106 and 107 (83 and 84 in CDK2) form van der Waals contacts with the benzylamino group. As in the CDK2 olomoucine complex, the Lys-112 side chain forms a hydrogen bond with the benzene ring and possibly contributes significantly to the binding affinity. Since this lysine is not conserved among protein kinases, it might also contribute to the binding specificity of olomoucine. Since the X-ray structure of ERK2 is of the inactive form of the enzyme, which shows different domain associations from the active cAPK structure, contacts to olomoucine might be slightly different in the active form of ERK2.

Although structural and functional data correlate well for cAPK and MAP kinase and identify the benzylamino group of olomoucine as a specificity confering group, we cannot identify a single feature of the kinase structure that is critical for olomoucine binding to protein kinases. For example, the predicted sterical hindrance in cAPK cannot explain the inability of other protein kinases without extensions, like CDK4, to bind olomoucine. CDK4 has a three-residue and eight-residue insertion between β3 and α1, and between β4 and β5, respectively, relative to CDK2. However, both insertions are far removed from the ATP binding pocket (Fig. 2) and most likely do not interfere with olomoucine binding. Of the CDK2 residues that contact the benzylamino group, Ile-10 and Leu-134 are conserved

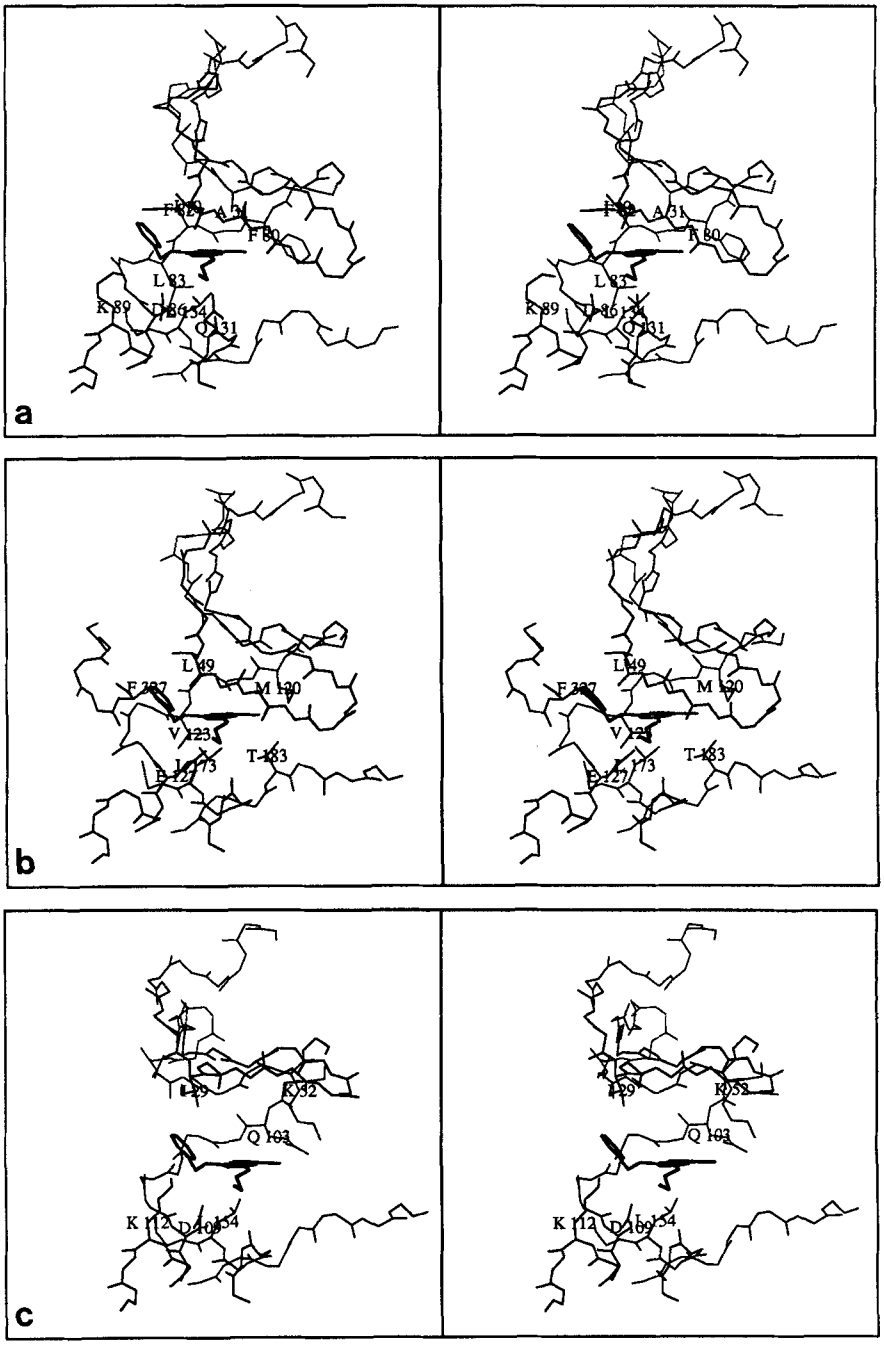

Fig. 8. Stereo diagrams of the binding pockets in CDK2 (**a**), cAPK (**b**), and ERK2 MAP–kinase (**c**). Olomoucine was placed into the binding pockets of cAPK and ERK2 by superimposing the CDK2–olomoucine complex onto the respective protein kinase structure. Resulting protein ligand contacts were calculated using CONTACSYM[37] and only side chains of contact residues are displayed. Other parts of the protein are shown in backbone representation and olomoucine in fat lines.

while residues 82 to 89 show several nonconservative sequence differences in CDK4. Without a three-dimensional structure for CDK4 available, it seems most likely that those sequence differences could affect olomoucine binding either directly through different side chain contacts or indirectly through backbone conformational changes. Supporting this thesis is the fact that CDK6, which is the closest relative to CDK4 with 70% sequence identify,[52] has also a very low affinity to olomoucine with an IC_{50} of >250 μM (Table III). Hence, a combination of steric obstructions and/or loss of favorable interactions due to differences in the backbone structure or sequence differences might account for the selectivity in different protein kinases.

In summary, the comparison of the three-dimen-

sional structures of the inhibitor–CDK2 complexes with the ATP–CDK2 complex shows that the hydrophobic adenine binding pocket of CDK2 has a surprising ability to accommodate different orientations of the purine ring. The identification of the benzylamino group of olomoucine and its contact residues in the kinases as critical for selective binding should prove useful in modifying and improving the lead compound. In addition, crystal structures of other olomoucine–kinase complexes could help us better understand the kinase features which are critical for olomoucine specificity.

ACKNOWLEDGMENTS

We thank Susan Taylor and Lynn Ten Eyck for cAPK coordinates and Elizabeth Goldsmith for ERK2 MAP kinase coordinates. This work was supported by a fellowship (to U.S.-G.) from the American Cancer Society, by grants (to S.-H. Kim) from the Department of Energy, by grants from the EEC (ERB3510PL920279) (to J. Vesely) and from the "Association pour la Recherche sur le Cancer" (ARC 6268) (to L. Meijer), and grants (to D.O. Morgan) from the NIH, the Markey Charitable Trust, the March of Dimes Birth Defects Foundation, and the Rita Allen Foundation.

REFERENCES

1. Norbury, C., Nurse, P. Animal cell cycles and their control. Annu. Rev. Biochem. 61:441–470, 1992.
2. Matsushime, H., Ewen, M.E., Strom, D.K., Kato, J.-Y., Hanks, S.K., Roussel, M.F., Sherr, C.J. Identification and properties of an atypical catalytic subunit ($p34^{PSK-J3}$/cdk4) for mammalian D type G1 cyclins. Cell 71:323–334, 1992.
3. Nigg, E.E. Targets of cyclin-dependent kinases. Curr. Opin. Cell. Biol. 5:187–193, 1993.
4. Gould, K.L., Moreno, S., Owen, D.J., Sazer, S., Nurse, P. Phosphorylation of Thr 167 is required for *Schizosaccharomyces pombe* $p34^{cdc2}$ function. EMBO J. 10:3297–3309, 1991.
5. Desai, D., Gu, Y., Morgan, D.O. Activation of human cyclin-dependent kinases in vitro. Mol. Biol. Cell 3:571–582, 1992.
6. Solomon, M.J., Lee, T., Kirschner, M.W. Role of phosphorylation in $p34^{cdc2}$ activation: Identification of an activating kinase. Mol. Biol. Cell 3:13–27, 1992.
7. Gu, Y., Rosenblatt, J., Morgan, D.O. Cell cycle regulation of CDK2 activity by phosphorylation of Thr160 and Tyr15. EMBO J. 11:3995–4005, 1992.
8. Connell-Crowley, L., Solomon, M.J., Wei, N., Harper, J.W. Phosphorylation independent activation of human cyclin-dependent kinase 2 by cyclin A in vitro. Molec. Biol. Cell 4:79–92, 1993.
9. Krek, W., Nigg, E.A. Mutations of $p34^{cdc2}$ phosphorylation sites induce premature mitotic events in HeLa cells: Evidence for a double block to $p34^{cdc2}$ kinase activation. EMBO J. 10:3331–3341, 1991.
10. Norbury, C., Blow, J., Nurse, P. Regulatory phosphorylation of the $p34^{cdc2}$ protein kinase in vertebrates. EMBO J. 10:3321–3329, 1991.
11. Parker, L.L., Atherton-Fessler, S., Piwnica-Worms, H. $p101^{wee1}$ is a dual-specificity kinase that phosphorylates $p34^{cdc2}$ on tyrosine 15. Proc. Natl. Acad. Sci. U.S.A. 89: 2917–2921, 1992.
12. McGowan, C.H., Russell, P. Human Wee1 kinase inhibits cell division by phosphorylating $p34^{cdc2}$ exclusively on Tyr15. EMBO J. 12:75–85, 1993.
13. Serrano, M., Hannon, G.J., Beach, D. A new regulatory motif in cell-cycle control causing specific inhibition of cyclin D/CDK4. Nature (London) 366:704–707, 1993.
14. Kamb, A., Gruis, N.A., Weaver-Feldhaus, J., Liu, Q., Harshman, K., Tavtigian, S.V., Stockert, E., Day III, R.S., Johnson, B.E., Skolnik, M.H. A cell cycle regulator potentially involved in genesis of many tumor types. Nature (London) 264:436–440, 1994.
15. Nobori, T., Miura, K., Wu, D.J., Lois, A., Takabayashi, K., Carson, D.A. Deletions of the cyclin-dependent kinase-4 inhibitor gene in multiple human cancers. Nature (London) 368:753–756, 1994.
16. Polyak, K., Lee, M.-H., Erdjument-Bromage, H., Koff, A., Roberts, J.M., Tempst, P., Massague, J. Cloning of $p27^{Kip1}$, a cyclin-dependent kinase inhibitor and a potential mediator of extracellular antimitotic signals. Cell 78:59–66, 1994.
17. Toyoshima, H., Hunter, T. p27, a novel inhibitor of G1 cyclin-CDK protein kinase activity, is related to p21. Cell 78:67–74, 1994.
18. Hengst, L., Dulic, V., Slingerland, J.M., Lees, E., Reed, S.I. A cell cycle-regulated inhibitor of cyclin-dependent kinases. Proc. Natl. Acad. Sci. U.S.A. 91:5291–5295, 1994.
19. Gu, Y., Turck, C.W., Morgan, D.O. Inhibition of CDK2 activity *in vivo* by an associated 20K regulatory subunit. Nature (London) 366:707–710, 1993.
20. Xiiong, Y., Hannon, G.J., Zhang, H., Casso, D., Kobayashi, R., Beach, D. p21 is a universal inhibitor of cyclin kinases. Nature (London) 366:701–704, 1993.
21. Harper, J.W., Adami, G.R., Wei, N., Keyomarsi, K., Elledge, S.J. The p21 Cdk-interacting protein cip1 is a potent inhibitor of G1 cyclin-dependent kinases. Cell 75: 805–816, 1993.
22. Dulic, V., Kaufmann, W.K., Wilson, S.J., Tisty, T.D., Lees, E., Harper, J.W., Elledge, S.J., Reed, S.I. p53-dependent inhibition of cyclin-dependent kinase activities in human fibroblasts during radiation-induced G1 arrest. Cell 76: 1013–1023, 1994.
23. Spruck III, C.H., Gonzalez-Zulueta, M., Shibata, A., Simoneau, A.R., Lin, M.-F., Gonzalez, F., Tsai, Y.C., Jones, P.A. p16 gene in uncultured tumours. Nature (London) 370: 183–184, 1994.
24. Hunter, T., Pines, J. Cyclins and cancer. Cell 66:1071–1074, 1991.
25. Keyomarsi, K., Pardee, A.B. Redundant cyclin overexpression and gene amplification in breast cancer cells. Proc. Natl. Acad. Sci. U.S.A. 90:1112–1116, 1993.
26. Wang, T.C., Cardiff, R.D., Zukerberg, L., Lees, E., Arnold, A., Schmidt, E.V. Mammary hyperplasia and carcinoma in MMTV-cyclin D1 transgenic mice. Nature (London) 369: 669–671, 1994.
27. Vesely, J., Havlicek, L., Strnad, M., Blow, J.J., Donella-Deana, A., Pinna, L., Letham, D.S., Kato, J.-Y., Detivaud, L., Leclerc, S., Meijer, L. Inhibition of cyclin-dependent kinases by purine derivatives. Eur. J. Biochem. 224:771–786, 1994.
28. DeBondt, H.L., Rosenblatt, J., Jancarik, J., Jones, H.D., Morgan, D.O., Kim, S.-H. Crystal structure of cyclin-dependent kinase 2. Nature (London) 363:595–602, 1993.
29. Rosenblatt, J., DeBondt, H., Jancarick, J., Morgan, D.O., Kim, S.-H. Purification and crystallization of human cyclin-dependent kinase 2. J. Mol. Biol. 230:1317–1319, 1993.
30. Furey, W., Swaminathan, S. "PHASES"—A program package for the processing and analysis of diffraction data from macromolecules. PA33. Am. Crystallogr. Assoc. Meeting Abstr. Ser. 2 18:73, 1990.
31. Brünger, A.T., Kuriyan, J., Karplus, M. Crystallographic R factor refinement by molecular dynamics. Science 235: 458–460, 1987.
32. Read, R.J. Improved Fourier coefficients for maps using phases from partial structures with errors. Acta Crystallogr. A42:140–149, 1986.
33. Brünger, A.T., Krukowski, A. Slow-cooling protocols for crystallographic refinement by simulated annealing. Acta Crystallogr. A46:585–593, 1990.
34. Jones, T.A. A graphics model building and refinement system for macromolecules. J. Appl. Crystallogr. 11:268–272, 1978.
35. Callahan, T., Gleason, W.B., Lybrand, T.P. *PAP:* A protein analysis package. J. Appl. Crystallogr. 23:434–436, 1990.
36. Rossmann, M.G., Argos, P. A comparison of the heme bind-

ing pocket in globins and cytochrome b_5. J. Biol. Chem. 250:7525–7532, 1975.
37. Sheriff, S., Hendrickson, W.A., Smith, J.L. Structure of myohemerythrin in the azidomet state at 1.7/1.3 Å resolution. J. Mol. Biol. 197:273–296, 1987.
38. Connolly, M.L. Analytical molecular surface calculation. J. Appl. Crystallogr. 16:548–558, 1983.
39. Ramachandran, G.N., Venkatchalam, C.M., Krimm, S. Stereochemical criteria for polypeptide and protein conformations. Biophys. J. 6:849–872, 1966.
40. Zheng, J., Knighton, D.R., Ten Eyck, L.F., Karlsson, R., Xuong, N.-H., Taylor, S.S., Sowadski, J.M. Crystal structure of the catalytic subunit of cAMP-dependent kinase complexed with MgATP and peptide inhibitor. Biochemistry 32:2154–2161, 1993.
41. Bossemeyer, D., Engh, R.A., Kinzel, V., Ponstingl, H., Huber, R. Phosphotransferase and substrate binding mechanism of the cAMP-dependent protein kinase catalytic subunit from porcine heart as deduced from the 2.0 Å structure of the complex with Mn^{2+} adenylyl imidodiphosphate and inhibitor peptide PKI(5–24). EMBO J. 12:849–859, 1993.
42. Hoppe, J., Freist, W., Marutzky, R., Shaltiel, S. Mapping the ATP-binding site in the catalytic subunit of adenosine-3′:5′-monophosphate-dependent protein kinase. Eur. J. Biochem. 90:427–432, 1978.
43. Burley, S.K., Petsko, G.A. Amino-aromatic interactions in proteins. FEBS Lett. 203:139–143, 1986.
44. Levitt, M., Perutz, M.F. Aromatic rings act as hydrogen bond acceptors. J. Mol. Biol. 201:751–754, 1988.
45. Janin, J., Chothia, C. The structure of protein-protein recognition sites. J. Biol. Chem. 265:16027–16030, 1990.
46. Wilson, I.A., Stanfield, R.L. Antibody-antigen interactions. Curr. Opin. Struct. Biol. 3:113–118, 1993.
47. Knighton, D.R., Zheng, J., Ten Eyck, L.F., Ashford, V.A., Xuong, N.-H., Taylor, S.S., Sowadski, J.M. Crystal structure of the catalytic subunit of cyclic adenosine monophosphate-dependent protein kinase. Science 253:407–414, 1991.
48. Bhatnagar, D., Roskoski Jr., R., Rosendahl, M.S., Leonard, N.J. Adenosine cyclic 3′,5′-monophosphate dependent protein kinase: A new fluorescence displacement titration technique for characterizing the nucleotide binding site on the catalytic subunit. Biochemistry 22:6310–6317, 1983.
49. Zheng, J., Trafny, E.A., Knighton, D.R., Xuong, N.-H., Taylor, S.S., Ten Eyck, L.F., Sowadski, J.M. 2.2 Å refined crystal structure of the catalytic subunit of cAMP-dependent protein kinase complexed with MnATP and a peptide inhibitor. Acta Crystallogr. D49:362–365, 1993.
50. Zhang, F., Strand, A., Robbins, D., Cobb, M.H., Goldsmith, E.J. Atomic structure of the MAP kinase ERK2 at 2.3 Å resolution. Nature (London) 367:704–711, 1994.
51. Zheng, J., Knighton, D.R., Xuong, N.-H., Taylor, S.S., Sowadsky, J.M., Ten Eyck, L.F. Crystal structures of the myristylated catalytic subunit of cAMP-dependent protein kinase reveal open and closed conformations. Protein Sci. 2:1559–1573, 1993.
52. Meyerson, M., Enders, G.H., Wu, C.-L., Su, L.-K., Gorka, C., Nelson, C., Harlow, E., Tsai, L.-H. A family of human cdc2-related protein kinases. EMBO J. 11:2909–2917, 1992.